Canadian
Journal of Physics

THE ELECTRICAL RESISTANCE OF DILUTE COPPER ALLOYS AT VERY LOW TEMPERATURES[1]

By GUY K. WHITE[2]

ABSTRACT

An adiabatic demagnetization cryostat for the measurement of electrical resistance of metals is described. Some preliminary results on copper containing small amounts of iron and tin are reported. These indicate that the rise in electrical resistance below the minimum is essentially complete in these specimens by $\backsim 2°$ K.

INTRODUCTION

Considerable work has been done in recent years on the problem of the anomalous minimum observed in the residual electrical resistance of some of the metallic elements (see, e.g., MacDonald (7) for references). This has generally been in the direction of investigating whether specific impurities or the presence of grain boundaries are necessary to produce a minimum in particular elements. MacDonald and Pearson (9) and Blewitt *et al.* (1) (cf. also Pearson (12)) have investigated the importance of various impurity elements and crystal structure in determining the position and depth of the minimum in copper.

Rather less research has been done on the behavior of the resistance at temperatures below that of the minimum to investigate whether the resistance continues to increase as the temperature is decreased and to determine the form of the temperature variation. Mendoza and Thomas (11) found that in high purity specimens of copper, silver, and gold which had a sensibly constant residual resistance or a rather shallow minimum in the liquid helium range, the resistance rose markedly at temperatures from 1° down to 0.1° K. Croft *et al.* (3), using a sample of gold of residual resistance comparable to the specimens of Mendoza and Thomas (viz. $\rho_{min}/\rho_{0°C.} \sim 10^{-2}$), found that the resistance continued to rise slowly at very low temperatures; they could represent the resistance by the relation

$$R \propto \log(\text{const}/T)$$

from liquid helium temperatures down to about 0.006° K., the increase appearing to be rather more uniform over the temperature range than in the case of Mendoza and Thomas.

In view of the availability of a wide range of dilute alloys in this laboratory
and the general interest in the transport properties of these alloys, it seemed
desirable to investigate the temperature variation of the resistance below the
minimum to see whether the sharp increase below 1° K. observed by Mendoza
and Thomas is confined to specimens of low residual resistance (i.e., containing
very small traces of impurity), and also to determine whether the resistance
of those alloys previously shown by MacDonald and Pearson to have a mini-
mum at 10 to 15° K. continues to increase noticeably below 1° K.

In the present note, some preliminary results are given on two such alloys
following a brief description of the apparatus used.

APPARATUS

The technique of compressing a paramagnetic salt round copper fins
(Mendoza (10)) has been used to provide the means for cooling specimens
below 1° K. and the very low temperatures produced were determined from
the mutual inductance by a ballistic deflection method (see Hull (5) for general
discussion).

The cryostat designed on these general principles is shown in Fig. 1. The
salt "pill", pressed round two 0.005 in. thick copper fins of total surface area
about 20 cm.^{2}, is $\frac{3}{8}$ in. in diameter and 2 in. long and is suspended from a light
brass frame by springs and nylon thread; the frame is a loose sliding fit in the
inner vacuum jacket.

The salt pill is painted with a thin layer of Glyptal lacquer to retard de-
hydration, immediately after being compressed, the salt consisting of cerium
magnesium nitrate in the preliminary experiments and more recently potassium
chrome alum.

Specimens in the form of a thin tape of the alloy approximately 1.0 mm.
× 0.1 mm. in section and 20 to 30 cm. in length are wound onto a "Formel"
covered copper cylinder W (0.5 cm. diameter × 2 cm. long) and coated with
"Formel" varnish. For ease in changing specimens, the end of this cylindrical
former is directly attached to a small copper block with parallel faces which
slips between the protruding copper fins and is clamped between them by a
screw; this provides good thermal contact between the two fins embedded in
salt and the copper former.

The electrical resistance of the specimen is measured by a galvanometer
amplifier (MacDonald (8)) on which the smallest voltage which can be de-
termined to ±0.2% is about 2 μv. Current and potential leads are attached
to the specimen tape by bismuth solder; the current leads are 32 B and S
manganin wire coated with a thin layer of lead (Pb) to make them super-
conducting and thus reduce Joule heating below 7° K.; the potential leads are
of "Formel"-enamelled 32 B and S manganin.

Coil S is the secondary of the mutual inductance and consists of a double
layer, 600 turn coil of 40 B and S copper wound on a bakelite former which
fits loosely round the salt pill. The primary P consists of about 1500 turns
of 36 B and S copper wire wound over an 8 in. length of the outer (brass)
vacuum case. The inner vacuum case, which is attached by Woods metal to

V

LIQUID HELIUM

LIQUID NITROGEN

C

HEATER

P

SALT

S

W

T
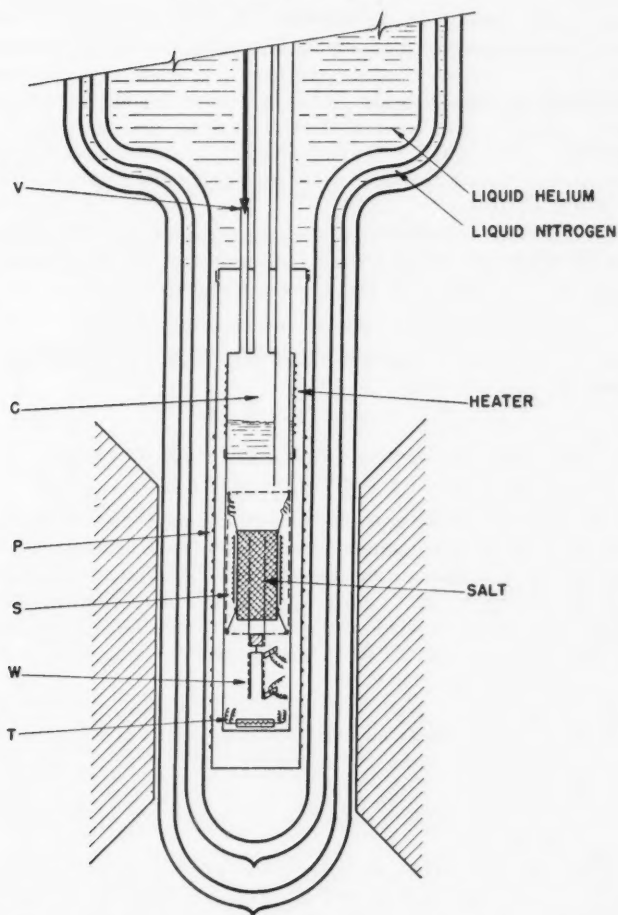
FIG. 1. Diagram of demagnetization cryostat for electrical resistance measurements.

the bottom of the copper chamber C, is of german-silver with vertical copper ribs silver-soldered to it so that uniformity of temperature along this case can be achieved without shielding the interior electrically.

At temperatures above 1° K., the inner enclosure is filled with a small pressure of helium exchange gas and the temperature is controlled by the following means: (i) 1 to 4.2° K.: filling chamber C with liquid helium through valve V and controlling the vapor pressure of the liquid helium by pumping through a manostat (Gilmont (4)); (ii) above 4.2° K.: supplying electrical heating to the empty chamber C sufficient to balance the loss of heat by conduction and radiation. The carbon resistance thermometer T in the inner

enclosure is calibrated in the region from 1 to 4° K., and may be then used to give the temperature (Clement and Quinnell (2)) in the higher temperature range.

To obtain temperatures below 1° K. the whole cryostat, mounted on a movable Hammond rack, is wheeled into the 3 in. gap between the $5\frac{3}{4}$ in. diam. pole faces of an A. D. Little electromagnet; the salt is then demagnetized in the usual way from a temperature of about 1.15° K. and field of approximately 17,000 oersteds.

All electrical leads were wound around the extensions of the pumping lines before being taken out through these lines and through an Apiezon W wax seal at the top of the cryostat, i.e., at room temperature.

TEMPERATURE MEASUREMENT BELOW 1° K.

The ballistic deflection method of measuring the mutual inductance is used, the deflection being given by

[1] $$\theta = [a/(T-\Delta)]+b$$

where a, b are constants depending on the coil geometry and

$$\Delta = ((4\pi/3)-D)fC .$$

f is the filling factor of the salt pill, C is the Curie constant per cc., which has a value of 0.0066 for potassium chrome alum (see Kurti and Simon (6) for discussion of the temperature measurement and evaluation of D), and D is the demagnetization factor. For a cylindrical pill of the dimensions used in this experiment, $D \simeq 1.3$. Thus assuming $f \simeq 1$, $\Delta \simeq 0.02°$ K. The constants a, b are found by plotting the deflection against the reciprocal of $(T-\Delta)$ in the region from 4° down to 1° K.

Equation [1] is valid at temperatures sufficiently above the Curie temperature that the salt behaves as an ideal paramagnetic. There appears to be no merit in trying to calculate the true thermodynamic temperature below 0.1° K. very accurately owing to the probability of small unknown temperature differences between the bulk of the salt and the specimen or copper-fin system (Mendoza (10, 11)).

The warm-up time in these experiments was of the order of one hour from the lowest temperature reached (salt temperature ~0.05° K.) to 0.5° K. The possibility that, with as short a warm-up time, the metallic specimens were not cooled to the indicated salt temperature has been checked in more recent experiments by Dugdale and MacDonald.* A suitable carbon resistance thermometer, calibrated in the liquid helium region (~1° and 4° K.), attached to the specimen showed that the temperature of the specimen fell below 0.3° K. almost immediately after demagnetization. The behavior of the carbon resistance thermometer made it an unreliable guide *below* this temperature; we can, however, say that the temperature of the salt as given by its susceptibility and the temperature of the metallic specimen should be in substantial agreement down to temperatures of this order.

*The author is indebted to Drs. J. S. Dugdale and D. K. C. MacDonald for this information. These experiments have also shown that the short warm-up time was due to inadequate thermal anchoring of the incoming electrical leads.

RESULTS

In Fig. 2 are shown the results of electrical resistance measurements on two annealed specimens of copper containing respectively 0.007 weight per cent tin and 0.056 weight per cent iron. Measurements below 1° K. on the
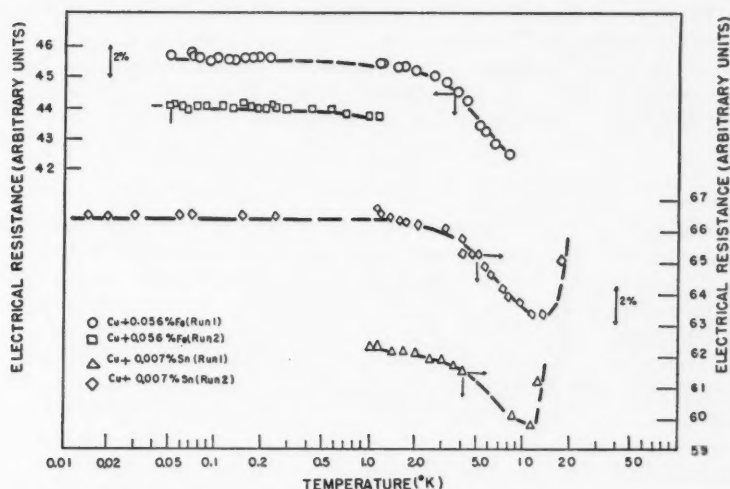
FIG. 2.   The variation of electrical resistance with salt temperature.

Cu–Sn alloy were made using cerium magnesium nitrate as cooling agent, and the salt temperatures are a little uncertain owing to the small ballistic deflections obtained in the calibrating region above 1° K.

The approximate residual resistance ratios, i.e., $\rho_{4.2}/(\rho_{295} - \rho_{4.2})$, for the two specimens having tin and iron impurities are 0.05 and 0.28, respectively. In the case of the Cu–Fe alloy, Run 1 and Run 2 were made using 10 ma. and 1 ma. measuring currents, the change producing no noticeable effect in the resistance–temperature relationship (Fig. 2).

The apparent separation (in arbitrary units) of the curves for Run 1 and Run 2 is a result of a slight change in over-all instrument sensitivity when the current range is altered. For the sake of clarity, the separation has been preserved rather than the usual current correction applied.

DISCUSSION AND CONCLUSION

Although these experiments are of a preliminary nature, they suggest that in copper alloys which have a minimum at relatively high temperatures (see MacDonald and Pearson (9) whose work on these alloys above 4° K. indicates that the minima occur in the region of 10 to 20° K.) the rise in resistance below the minimum becomes small as the temperature falls below 2 or 3° K. Below 1° K. no variation greater than the experimental error of resistance measurement (∼ 0.2%) was found.

It is hoped to investigate the resistance variation in this temperature range of higher purity specimens of copper and other monovalent metals in the near future.

ACKNOWLEDGMENTS

The writer is grateful to Dr. H. Preston-Thomas for his considerable assistance during the initial stages of design and assembly of the cryostat, to Drs. D. K. C. MacDonald and W. B. Pearson for discussion and providing the specimens which were investigated, and to Drs. R. P. Hudson and E. Ambler for advice on demagnetization techniques.

REFERENCES

1. BLEWITT, T. H., COLTMAN, R. R., and REDMAN, J. K.   Phys. Rev. 93: 891.   1954.
2. CLEMENT, J. R. and QUINNELL, F. H.   Rev. Sci. Instr. 23: 213.   1952.
3. CROFT, A. J., FAULKNER, E. A., HATTON, J., and SEYMOUR, E. F. W.   Phil. Mag. 44: 289. 1953.
4. GILMONT, R.   Anal. Chem. 23: 157.   1951.
5. HULL, R. A.   Phys. Soc. Cambridge Conference Report, p. 72.   1947.
6. KURTI, N. and SIMON, F. E.   Phil. Mag. 26: 849.   1938.
7. MACDONALD, D. K. C.   Phys. Rev. 88: 148.   1952.
8. MACDONALD, D. K. C.   J. Sci. Instr. 24: 232.   1947.
9. MACDONALD, D. K. C. and PEARSON, W. B.   In course of publication.   1955.
10. MENDOZA, E.   Ceremonies Langevin-Perrin.   Paris.   1948.   p. 53.
11. MENDOZA, E. and THOMAS, J. G.   Phil. Mag. 42: 291.   1951.
12. PEARSON, W. B.   Phil. Mag. 45: 1087.   1954.

PREDISSOCIATIONS OF THE C¹²O AND C¹³O MOLECULES¹

By A. E. Douglas and C. K. Møller²

ABSTRACT

The Ångström bands of C¹²O and C¹³O have been photographed with a high dispersion spectrograph and the predissociations previously reported in these bands have been re-examined. The predissociations provide good evidence that C¹²O has a dissociation limit 89595 ± 30 cm.$^{-1}$ above the $v = 0$ level of the ground state. The fourth positive $(A^1\Pi - X^1\Sigma)$ bands have been re-examined and it has been shown that, contrary to earlier reports, there is no evidence for predissociation in the $A^1\Pi$ state.

1. INTRODUCTION

The dissociation energy of CO is a quantity of importance not only for its own sake but also because it is related directly to the value of the latent heat of sublimation of carbon. Numerous studies of the CO spectrum have been made in attempts to determine the positions of two or more dissociation limits from which the dissociation energy can be derived and indeed it has been claimed that two such limits have been found near 9.6 and 11.1 ev. This claim has not been accepted without reservations and it has appeared desirable to re-examine the spectrum of CO in an attempt to obtain further information regarding these dissociation limits.

The best evidence for the 11.1 ev. dissociation limit has been obtained from predissociations in the $B^1\Sigma$ state. Coster and Brons (1) observed bands of the $B^1\Sigma - A^1\Pi$ (Ångström) system with $v' = 0$ and found that lines originating from rotational levels of the B state with J greater than 37 were much weaker than lines originating from lower levels. They attributed this effect to a predissociation in the $B^1\Sigma$ state. Later Schmid and Gerö (6) confirmed the work of Coster and Brons and also observed a similar predissociation in bands originating in the $v' = 1$ levels. The bands arising from the $v = 1$ levels are weak and Schmid and Gerö were able to observe the intensity change only in the P branches of the 1–0 band and in the Q branch of the 1–1 band.

A second predissociation near 11.1 ev. occurs in the $b^3\Sigma$ state and is observed in the $b^3\Sigma - a^3\Pi$ bands. The predissociations occur at higher J values than in the corresponding bands of the singlet state and therefore are not as valuable in determining the position of a dissociation limit.

The much-discussed 9.6 ev. predissociation in CO is reported to occur in the $A^1\Pi$ state. Gerö (3) observed bands of the $A^1\Pi - X^1\Sigma$ system (fourth positive system) and found a weakening of a number of lines in bands originating in the $v = 7$, 8, and 9 levels. The change in intensity of the lines is small and occurs over only a few rotational levels. In spite of the fact that a clear proof that predissociations do exist at these energies would at once establish the dissociation energy of CO to be 9.6 ev. or less, no spectra other than those originally obtained by Gerö have been forthcoming to substantiate

their existence. Both Herzberg (5) and Gaydon (2) have mentioned that they have been unable to confirm the existence of these predissociations.

The observed weakening of the lines in the Ångström bands is almost certainly due to a predissociation and the interpretation given by Gerö, which placed a dissociation limit at 11.1 ev., has been generally accepted. Hagstrum (4), however, from his electron impact results arrived at the value of 9.6 ev. for $D(CO)$ and has attempted to show that the spectroscopic results can be reinterpreted in a way to be consistent with this value. He has assumed that the weakening of the lines of the Ångström bands was caused by a predissociation involving a potential hill (Herzberg's type Ic predissociation) and that the dissociation limit is about 0.2 ev. below the observed predissociation in the $v = 0$ levels of the $B^1\Sigma$ state. In order to maintain this conclusion, Hagstrum was forced to assume either that the predissociation in the $v = 1$ level reported by Gerö was not real or that it was a predissociation unrelated to the one observed in the $v = 0$ level.

In order to obtain more definite experimental evidence regarding the predissociations of CO, we have photographed the Ångström bands of $C^{12}O$ and $C^{13}O$ and the fourth positive bands of $C^{12}O$ at high dispersion. The states of $C^{13}O$ should show the effects of predissociation at the same energy as the corresponding states of $C^{12}O$, but perturbations in the $C^{12}O$ and $C^{13}O$ spectrum will, in general, be quite different. Therefore, the study of the $C^{13}O$ spectrum should allow a clear differentiation between perturbations and predissociations and at the same time give confirmation of any real dissociation limits found in $C^{12}O$.

2. EXPERIMENTAL

The Ångström bands of CO were excited in a discharge through O_2 in a tube containing some carbon deposits. The carbon may readily be deposited by passing a discharge through methane in the tube. The Ångström bands of $C^{13}O$ were obtained by using $C^{13}H_4$* as the source of carbon and were photographed with a 21 ft. concave grating spectrograph at a dispersion of 2.5 Å/mm. The corresponding bands of $C^{12}O$ were photographed with a 35 ft. spectrograph at a dispersion of 0.7 Å/mm. The fourth positive bands of CO were excited first in the same discharge as was used for the Ångström bands and later in a very low pressure discharge in streaming CO_2 excited by a high frequency oscillator. The bands were photographed in the third order of the 35 ft. spectrograph at a dispersion of about 0.23 Å/mm.

3. RESULTS

The Ångström bands of $C^{12}O$ were not measured, but the lines could readily be identified from the measurements of Schmid and Gerö. The effects of predissociation were found in the bands at the positions previously reported by Coster and Brons (1) and by Schmid and Gerö (6). A portion of the 1–0 band reproduced in Fig. 1a shows the weakening of the lines in the P, Q, and R branches. It is difficult to show all three branches on the same reproduction

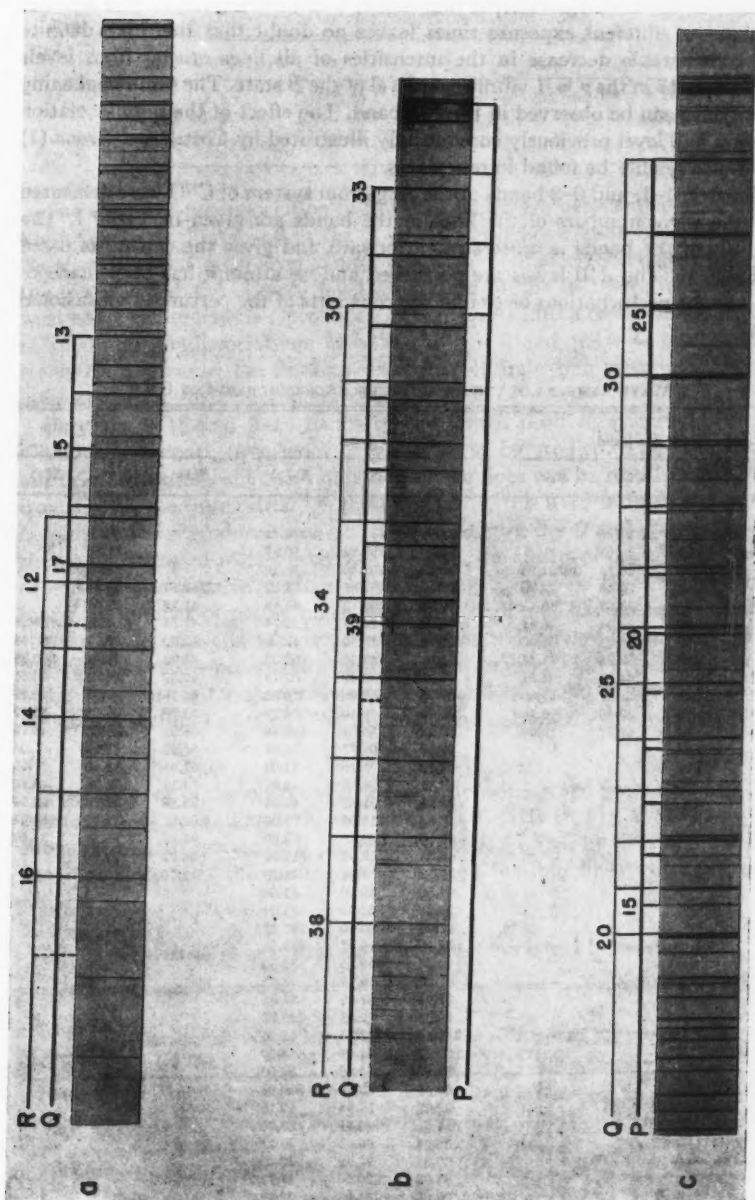*The $C^{13}H_4$ was supplied by Professor K. Clusius.

Fig. 1.

because of their widely different intensities, but an examination of a number of plates of different exposure times leaves no doubt that there is a definite and considerable decrease in the intensities of all lines arising from levels above $J = 17$ in the $v = 1$ vibrational level of the B state. The same weakening of the lines can be observed in the 1–1 band. The effect of the predissociation in the $v = 0$ level previously convincingly illustrated by Coster and Brons (1) could also readily be found in our plates.

The 0–1, 1–1, and 0–2 bands of the Ångström system of $C^{13}O$ were measured and the wave numbers of the lines in the bands are given in Table I. The analysis of the bands is quite straightforward and gives the constants listed in Table II. The $A^1\Pi$ levels are perturbed and no attempt has been made to analyze the perturbations or to find the constants of the perturbed vibrational levels.

TABLE I

WAVE NUMBERS OF THE LINES OF THE ÅNGSTRÖM BANDS OF $C^{13}O$

J	0–1 Band			0–2 Band			1–1 Band		
	$P(J)$	$Q(J)$	$R(J)$	$P(J)$	$Q(J)$	$R(J)$	$P(J)$	$Q(J)$	$R(J)$
0									
1	20709.48	20713.20		19294.01		19305.21		22750.40	
2	07.17	14.63		91.79	19299.24	10.42		51.69	
3	05.54	16.74	20731.66	90.29	301.46	16.40		53.73	
4	04.57	19.56	37.96	89.55	04.47	23.12	22741.54	56.36	
5	04.57	23.03	45.43	89.55	08.19	30.49	41.28	59.65	
6	04.98	27.34	53.39	90.29	12.67	38.74	41.54	63.56	22789.25
7	06.20	32.31	62.05	91.79	17.98	47.69	42.50	68.17	797.58
8	08.14	37.96	71.44	94.01	23.66	57.33	43.99	73.44	806.38
9	10.78	44.30	81.51	97.00	30.49	67.73	46.32	79.35	16.05
10	14.13	51.37	92.30	300.70	37.90	78.91	49.20	85.95	26.36
11	18.16	59.16	803.76	05.21	46.10	90.79	52.78	93.22	37.22
12	23.03	67.72	15.98	10.42	55.04	403.48	56.99	801.20	48.79
13	28.45			16.40	64.77	16.83	61.90	10.83	61.04
14	34.78			23.12	75.16	31.02	67.54	18.20	73.99
15	42.20			30.49	86.34	45.90	74.39	28.24	88.10
16				38.74	98.25	61.51	78.89	38.79	99.94
17				47.69	410.95	77.95	87.11	49.99	915.48
18				57.50	26.75	95.06	95.42	61.99	31.04
19				68.03	38.57	512.97	804.22	72.90	
20				79.23	53.43	31.59	13.70		
21				91.30	69.20	51.04			
22				404.20	85.69	71.21			
23				17.95	502.90	92.37			
24				33.19	20.97	615.01			
25				43.25	39.85	32.38			
26				61.00	59.78	57.52			
27				77.95	81.29	81.86			
28				95.52	92.88	706.72			
29				513.78	618.55	32.26			
30				32.97	41.97	58.79			
31				53.98	65.60	87.08			
32				69.55	89.90	809.98			
33				92.37	14.94	40.10			
34				614.01	40.11	69.06			
35				36.94	66.43	99.27			
36				60.86	93.99	930.48			
37				83.00	820.30	59.72			
38				08.90	51.25	92.98			
39				35.14	78.55				
40				61.77					

TABLE II

CONSTANTS OF THE ÅNGSTRÖM BAND OF $C^{13}O$

Band	ν_0	B'	D'
0–1	20712.50	1.863	5.4×10^{-6}
0–2	19297.00	1.863	
1–1	22749.76	1.837	

The effects of predissociation in the $C^{13}O$ bands are very similar to those in the $C^{12}O$ bands. For $v = 0$ in the B state the predissociation occurs between the $J = 39$ and $J = 40$ level and for $v = 1$ the predissociation occurs between the $J = 19$ and the $J = 20$ level. A section of the 0–2 band showing the weakening of the lines is reproduced in Fig. 1b. As in the corresponding bands of $C^{12}O$, the predissociations in both the $v = 0$ and the $v = 1$ vibrational levels do not cause the lines to disappear entirely but merely reduce the intensity of the lines by a factor of about two.

Only the 9–18 and 9–19 bands of the fourth positive system have been obtained sufficiently free from overlapping to be studied. The bands have not been measured, but the numbering of the lines can be readily established from Gerö's measurements. Of the two bands, the 9–19 is freer from over-lapping and is reproduced in Fig. 1c. In this figure the Q and P branches are shown in the region where, according to Gerö, the effects of the predissociation should be evident. No noticeable weakening of any of the lines has been found. A number of plates taken with both high and low pressures of O_2 in the discharge tube and with a very low pressure discharge through CO_2 have been examined. On none of the plates is there any evidence of predissociation. Since no evidence for the predissociation could be found in the $C^{12}O$ bands, the corresponding bands of $C^{13}O$ were not photographed.

4. DISCUSSION

The positions of the observed predissociations measured from the vibration-less ($v = -\frac{1}{2}$) ground state are shown in Table III. In Fig. 2 the energy at the point of predissociation is plotted against $J(J+1)$. The $C^{12}O$ and the $C^{13}O$ data are plotted on the same graph. Through the four lines which represent

TABLE III

POSITIONS OF THE OBSERVED PREDISSOCIATIONS IN THE $B^1\Sigma$ STATES
OF $C^{12}O$ AND $C^{13}O$

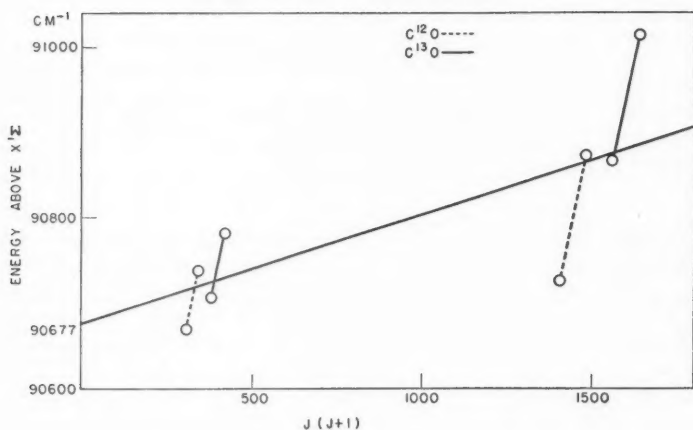| Molecule	Vibrational states	J value of last strong line	J value of first weak line	Rotational energy	Energy above the vibrationless $X^1\Sigma$ state
$C^{12}O$	0	37	—	2726.4	90726.0
$C^{12}O$	0	—	38	2873.1	90872.7
$C^{12}O$	1	17	—	587.3	90669.1
$C^{12}O$	1	—	18	656.3	90738.1
$C^{13}O$	0	39	—	2893.1	90866.0
$C^{13}O$	0	—	40	3040.8	91013.7
$C^{13}O$	1	19	—	697.7	90707.9
$C^{13}O$	1	—	20	771.0	90781.2

FIG. 2.

the energy range in which the predissociation must occur, a "limiting" curve (here a straight line) has been drawn and extrapolated to $J = 0$. The fact that one smooth line can pass through both the $C^{12}O$ and the $C^{13}O$ points shows that interpretation of the weakening of the lines as a predissociation is a reasonable one, and does much to eliminate any slight possibility that the observed effect is due to perturbation.

The theory of predissociations and the limiting curve has been given by Herzberg and will not be discussed in detail here. The theory shows that the limiting curve need not be, and indeed probably should not be, a straight line and also that the slope of the curve should not be the same for $C^{12}O$ and $C^{13}O$. The expected difference in slope of the $C^{12}O$ and $C^{13}O$ curves is very small and can be neglected here. Since the observed data are insufficient to determine the shape of the curve, a straight line is probably the best approximation that can be made. The theory shows that the slope of this straight line is equal to or greater than that of the true curve at the intercept.

From the slope of the limiting curve it is possible to determine whether the predissociation takes place at a dissociation limit or over a potential hill. The slope of the curve at the intercept is $h/8\pi^2 c\mu r^2$ where $h/8\pi^2 c$ is a constant, μ is the reduced mass of the molecule, and r is the internuclear distance of any potential hill over which the predissociation occurs. From the slope of the straight line in Fig. 2, it follows that $r \simeq 5$ Å. As pointed out above, this slope may be too great. Thus it follows that if any potential hill exists, it must occur at an internuclear distance of 5 Å or greater. Clearly, at this large internuclear distance, the interaction between the O and C atom is negligibly small and the potential hill, if one exists, must be correspondingly small.

The intercept on the $J = 0$ axis in Fig. 2 is at 90677 cm.$^{-1}$ with an estimated error of ± 30 cm.$^{-1}$. A dissociation limit of CO must therefore exist 90677 ± 30 cm.$^{-1}$ above the vibrationless ($v = -\frac{1}{2}$) ground state or, for $C^{12}O$, allowing

for the zero point energy, a dissociation limit is 89595 ± 30 cm.$^{-1}$ (11.1078 ± 0.0037 ev.) above the $v = 0$ level of the ground state. This latter value agrees well with the value of 89620 ± 50 cm.$^{-1}$ given by Schmid and Gerö (6).

As discussed earlier, Hagstrum has considered the dissociation limit in CO to be about 300 cm.$^{-1}$ below 89595 cm.$^{-1}$. He considered either that the existence of a predissociation in the $v = 1$ level of the B state was not well established experimentally, or that the predissociation did exist but was not related to the predissociation in the $v = 0$ level. The present experimental work shows that the weakening of the lines in the bands originating in the $v = 1$ vibrational state is as definite as and in fact very similar to that observed in the bands originating in the $v = 0$ state. This fact has been confirmed for both the $C^{12}O$ and the $C^{13}O$ bands. The predissociation in the $v = 1$ state can therefore not be disregarded. The possibility that the predissociations in the $v = 1$ and the $v = 0$ states are unrelated also seems remote. Aside from the improbability that two unrelated predissociations in the same electronic state should fall so close together, the very similar appearance of the two predissociations gives a strong indication that they are related. Both in bands originating from the $v = 0$ and from the $v = 1$ levels, the predissociation does not cause the spectrum to break off completely, but only reduces the intensity of the lines by a factor of about two; that is, the probability of dissociating the molecule is, in each case, about equal to the probability of radiation. The ratio of the probability of decomposition to the probability of radiation may vary over many orders of magnitude from one predissociation to another and the fact that this ratio is nearly the same for the observed predissociation in the $v = 0$ and the $v = 1$ levels gives a strong indication that they are related. There therefore now appears little evidence to support Hagstrum's interpretation of the predissociation of the $B^1\Sigma$ state.

As mentioned earlier, we have been unable to confirm the existence of a predissociation in the ninth vibrational level of the $A^1\Pi$ state. Indeed we have been able to show that bands originating in this level show no predissociation. It is probable that the apparent weakening of a number of lines in these bands found by Schmid and Gerö results from overlapping lines or some other spurious effect. We believe that there now exists no evidence for predissociations in the CO spectrum below 89595 cm.$^{-1}$.

The present work has confirmed the existence of a dissociation limit in $C^{12}O$ at 89595 cm.$^{-1}$ but has given no information regarding the states of the atoms resulting from the dissociation. Kronig's selection rules for predissociation are of little assistance in giving information about the possible states of the atoms since the predissociation is a weak one and therefore possibly a forbidden one. The possible states of the atoms and the resulting values of $D_0(C^{12}O)$ are given in Table IV. It can be seen from this table that, owing to the triplet splitting of the ground states of the carbon and oxygen atoms, there is an almost continuous range of possibilities between 89595 and 89325 cm.$^{-1}$, a second range between 79401 and 79175 cm.$^{-1}$, and a third between 73727 and 73684 cm.$^{-1}$. It appears quite possible that in the near future non-spectroscopic and perhaps additional spectroscopic work will establish within which

TABLE IV

POSSIBLE VALUES OF $D_0(C^{12}O)$

States of the atoms at the 89595 cm.$^{-1}$ limit		$D_0(C^{12}O)$ (cm.$^{-1}$)
C	O	
$^3P_0$	$^3P_2$	89595
$^3P_1$	$^3P_2$	89579
$^3P_2$	$^3P_2$	89552
$^3P_0$	$^3P_1$	89436
$^3P_1$	$^3P_1$	89420
$^3P_2$	$^3P_1$	89393
$^3P_0$	$^3P_0$	89368
$^3P_1$	$^3P_0$	89352
$^3P_2$	$^3P_0$	89325
$^1D_2$	$^3P_2$	79401
$^1D_2$	$^3P_1$	79243
$^1D_2$	$^3P_0$	79175
$^3P_0$	$^1D_2$	73727
$^3P_1$	$^1D_2$	73711
$^3P_2$	$^1D_2$	73684

of these three ranges the true value lies. It will, however, be very difficult to determine the value of $D_0(CO)$ within the range of values resulting from the triplet splittings of the atomic states.

ACKNOWLEDGMENT

REFERENCES

1. COSTER, D. and BRONS, F. Physica, 1: 155. 1934.
2. GAYDON, A. G. Dissociation energies and spectra of diatomic molecules. Chapman and Hall, Limited, London. 1953.
3. GERÖ, L. Z. Physik, 100: 374. 1936.
4. HAGSTRUM, H. D. Phys. Rev. 72: 947. 1947.
5. HERZBERG, G. Spectra of diatomic molecules. Vol. II. D. Van Nostrand Company, Inc., New York. 1950.
6. SCHMID, R. and GERÖ, L. Z. Physik, 93: 656. 1935.

THE HALF-LIFE OF Sr[90][1]

BY D. M. WILES[2] AND R. H. TOMLINSON

ABSTRACT

The value of 27.7 ± 0.4 years has been obtained for the half-life of Sr[90] from the absolute disintegration rate of a known number of atoms. The disintegration rate was measured with a 4π proportional counter and the number of atoms was determined with a mass spectrometer using isotope dilution.

INTRODUCTION

While Sr[90] with its daughter Y[90] is one of the most important radioisotopes occurring in fission products more than two years old, there is still some question as to its half-life. The value announced shortly after Sr[90] had been first reported in 1943 was 30 yr. (1) and somewhat later the value 25 yr. (2) was accepted. The currently accepted value (4, 7) of 19.9 ± 0.3 yr. was obtained in 1950 by Powers and Voigt (9) using a Lauritsen electroscope and decay with time studies over a period of seven years. Since this is only a small fraction of the half-life, it would seem that the alternative approach utilizing the rate of disintegration of a known mass of the substance might be more accurate. This latter method, used extensively for long-lived isotopes, has recently been employed in the determination of the half-life of 73.6-yr. U[232] (11). In the present investigation a 4π proportional counter has been used to measure the absolute disintegration rate of a Sr[90] solution and a 90° solid source mass spectrometer to determine its concentration.

EXPERIMENTAL

Counting Techniques

The 4π counter used was made in this laboratory and its general construction is substantially the same as commercial models and others described in the literature (3). Samples were mounted on V.Y.N.S. (polyvinylchloride-acetate copolymer) films fastened across the circular opening (diameter 2.5 cm.) in disks (diameter 5.8 cm.) made from 0.005 in. sheet nichrome. The central hole was large enough so that the metal of the disk would subtend a solid angle of less than 1% of 4π steradians. The effective geometry of the counter for β particles would be 4π steradians since most of the betas which strike the source mount would be expected to trigger the counting circuit.

The films themselves were made by "stretching" a solution of V.Y.N.S. in cyclohexanone on the surface of water to a thickness ranging from 140 to 210 mμ (i.e. 20 to 30 μgm. per sq. cm. superficial density) according to the technique developed by Pate and Yaffe (8). Since a poorly conducting film reduces the counting rate for a given source and results in the loss of voltage plateau (3), the films were sputtered with gold on one side to a thickness of 5 to 10 μgm. per sq. cm., the criterion of coverage being conductivity. Thick-

nesses of both plastic and gold films were estimated by means of interference patterns as described by Pate and Yaffe (8).

The counter was a continuous gas flow type operated at one atmosphere of C.P. methane; the electronic system included a non-overloading linear amplifier. The voltage plateau characteristics of this counter were studied and the plateau showed no measurable slope between 3000 and 3250 v. The dead-time of the complete system, as fixed by the RC input circuit of the linear amplifier, was found to be 2.5×10^{-4} sec. and the background was of the order of one pulse per second.

Counting Corrections and Calibration of Counter

In addition to the corrections for coincidence loss and background, it was necessary to consider other possible corrections. Seliger and Cavallo (10) have shown that the absorption loss in the source mount is given by

$$N_0 = N_{TB}/(1 - \tau/2)$$

where N_0 = the absolute counting rate,

$\tau = (N_T - N_B)/(N_{TB} - N_B)$, i.e. the fractional absorption in the film,

T and B refer to the upper and lower halves of the counter.

This equation gave an over-all correction of approximately 0.2% for Sr^{90} and Y^{90} in equilibrium. Mann and Seliger (5) have shown that neglect of backscatter in this relation introduces an uncertainty never greater than 1.5%. Consequently no adjustment of the measured disintegration rates was made because it would have had no significance when compared to the limits imposed by sample preparation.

Self-absorption in the source itself would, of course, result in an undesirable reduction of the counting rate but this can be kept to a negligible minimum by using carrier-free nuclides. Since the quantity of strontium on any one film was of the order of 10^{-12} gm., which even with a microgram of inherent impurities would result in negligible self-absorption, it was assumed that there was no reduction of the counting rate as a result of finite source thickness.

Hawkings *et al.* (3) have shown how sample position affects the efficiency of the counter. Their data indicate that for a methane-filled counter, no correction for this effect would be required for the conditions used in this work.

The efficiency of the counter was tested by means of P^{32} and Au^{198} solution standards from the National Bureau of Standards. The results of this series of measurements are shown in Table I. Since each count represents a separate dilution from the standard solutions, the deviations from the average represent uncertainties in the sampling technique. These values have been corrected for radioactive decay using 14.60 days (13) for the half-life of P^{32} and 2.69 days for the half-life of Au^{198} (12). Counts were taken through two half-lives of P^{32} and through eight half-lives of Au^{198}. On the basis of these measurements the counter was assumed to be more than 99% efficient for β particles in this energy range.

TABLE I

CALIBRATION OF COUNTER WITH SOLUTION STANDARDS

	P^{32}		Au^{198}	
Sample	Disintegrations per second per ml. $\times 10^{-6*}$		Sample	Disintegrations per second per ml. $\times 10^{-5*}$
1	159		1	3.80
2	159		2	3.85
3	163		3	4.01
4	160		4	3.82
5	160		5	3.89
6	157		6	3.84
Average	$160 \pm 1\%$		Average	$3.87 \pm 2\%$
N.B.S. value	$160 \pm 2\%$		N.B.S. value	$3.84 \pm 3\%$

Corrected to zero time and for coincidence loss and background.

Mass Spectrometry

The concentration determinations were carried out by isotope dilution techniques using a 90° sector mass spectrometer with magnetic scanning and a hot filament ion source. The filaments, made from tungsten ribbon, were platinum-plated and then heated for approximately one hour under vacuum at about 2000°C. Sample solutions were evaporated on teflon under a heat lamp to a volume of approximately 30 μl., then transferred and evaporated on to the filament.

The isotope dilution method for finding the concentration was carried out as follows. The ratio of Sr^{88} to Sr^{90} in the solution was measured; a known amount of Sr^{88} (about 0.125 μgm.) was added to 1 ml. of solution and the ratio was measured again. These mass spectrometric ratios and the weight of added Sr^{88} were then utilized to obtain the amount of Sr^{90}.

Solution Handling

The Sr^{90} for both the counting and mass spectrometry came from a solution containing about 0.1 μgm./ml. of fission product Sr^{90}. Since the sample was over three years old, the 55-day Sr^{89} originally present would have decayed to the extent that its contribution to the activity was less than 0.1% of the total. One gram of solution was weighed out directly for the mass spectrometric determinations but more dilute solutions were necessary in order that a measurable volume could be used for counting.

Aliquots of 100 μl. were measured with a Gilmont ultramicroburette which, on recalibration using a semimicrobalance, was proved to have a reproducibility of 1 μl. Adsorption losses of the carrier-free strontium from solution could have led to serious errors. To minimize these losses, all glassware used was coated with "desicote" and all solutions were kept acidic. In order to test for fractionation, yttrium carrier was added to some solutions used for counting, strontium carrier was added to others. Further tests were carried out by using Sr^{88} solutions of widely differing concentrations for isotope dilution.

RESULTS AND DISCUSSION

Table II shows the activity of the solution containing Sr^{90} and Y^{90} in equilibrium proportions. The values for samples 1, 2, and 3 are equilibrium counting rates obtained 300 hr. after sample preparation. A change in count

TABLE II

ACTIVITY OF SOLUTION CONTAINING Sr^{90} AND Y^{90} IN EQUILIBRIUM

Sample	Disintegrations/sec. on film*	Disintegrations/sec./ml. of Sr^{90}–Y^{90} equilibrium solution $\times 10^{-6}$
1	57.20	1.327
2	57.36	1.331
3	56.81	1.320
4	51.34	1.334
5	51.30	1.332
	Average	1.329±0.006

*Corrected for coincidence loss and background but not for aliquot size.

with time for these samples showed that Y^{90}, adsorbed during sample preparation, was regaining its equilibrium concentration. Sample 4 was taken from a solution to which yttrium carrier had been added and sample 5 contained both strontium and yttrium carrier; these showed no change in counting rate with time.

Table III shows the agreement between the concentration values obtained in this investigation (numbers 1, 2, and 3) and those obtained by other experimenters in the same laboratory (numbers 4 and 5). Values 1 and 2 were

TABLE III

CONCENTRATION OF Sr^{90} SOLUTION

Value	Micrograms of Sr^{90} per ml. of solution
1	0.127
2	0.124
3	0.123
4	0.125
5	0.123
Average	0.124±0.002

obtained using a solution containing 1 μgm. per ml. of Sr^{88} for isotope dilution whereas 3, 4, and 5 were obtained using Sr^{88} solution of concentration 0.1 μgm. per ml. Since no systematic difference is noted in the values obtained from these different conditions, it may be concluded that adsorption losses have been kept to negligible proportions for strontium solutions having concentrations down to 0.1 μgm. per ml. In the solutions used for counting, neither strontium nor yttrium carrier added to the initial aliquot resulted in a

change in the value obtained, and hence adsorption of strontium has also been considered negligible in the preparation of the counting slides.

The limits of error shown in Tables II and III are the standard deviations of the independently determined values in each table and are considered to represent limits imposed by the measurement of small volumes of solution.

Knowing the number of atoms present (n) and the rate of disintegration (dn/dt), one can calculate the half-life using the relationship

[1] $$dn/dt = -n\lambda$$

where $$\lambda = 0.6932/\text{half-life}.$$

The average values for the activity and the concentration taken from Tables II and III give a half-life of 27.7 yr. $\pm$ 0.4 yr.

Fission yield studies of U^{235} provide evidence for choosing between the currently accepted value of 19.9 yr. obtained by Powers and Voigt (9) and the 27.7 yr. obtained in this work. It follows from equation [1] that the fission yield of Sr^{90} may be evaluated from a determination of the Sr^{90} disintegration rate corresponding to a given amount of U^{235} fissions. Glendenin's value of 25 yr. (2) for the half-life of Sr^{90} assumed the yield of this isotope to lie on a smooth fission yield curve. The 19.9-yr. half-life would lead to a fission yield some 20% lower whereas the 27.7-yr. half-life would correspond to a value about 11% above the smooth yield curve. Preliminary work in this laboratory shows that the fission yield of Sr^{90} is high and that the corresponding fission fragment of mass 144 has a yield about 7% above the smooth fission yield curve (6). These data tend to support the value of 27.7 $\pm$ 0.4 yr. for the half-life of Sr^{90}.

ACKNOWLEDGMENT

REFERENCES

1. CORYELL, C. D.   Plutonium Project Report, CC-112. December 1943. p. 15.
2. GLENDENIN, L. E.   Further Studies of Sr^{90} and Y^{90}, NNES-PPR, 9B, Paper No. 7.11.2. 1946.
3. HAWKINGS, R. C., MERRITT, W. F., and CRAVEN, J. H.   Proceedings of Symposium, Maintenance of Radioactive Standards. N.P.L. May 1951.
4. HOLLANDER, J. M., PERLMAN, I., and SEABORG, G. T.   Revs. Mod. Phys. 25: 469.   1953.
5. MANN, W. B. and SELIGER, H. H.   J. Research Natl. Bur. Standards, 50: 197.   1953.
6. MELAIKA, E. A., PARKER, M. J., PETRUSKA, J. A., and TOMLINSON, R. H.   Unpublished data.
7. Nuclear Data. Supplement 2 to N.B.S. Circular 499. U.S. Department of Commerce, N.B.S.   1951.
8. PATE, B. D. and YAFFE, L.   Can. J. Chem. 33: 15.   1955.
9. POWERS, R. I. and VOIGT, A. F.   Phys. Rev. 79: 175.   1950.
10. SELIGER, H. H. and CAVALLO, L.   J. Research Natl. Bur. Standards, 47: 41.   1951.
11. SELLERS, P. A., STEVENS, C. M., and STUDIER, M. H.   Phys. Rev. 94: 952.   1954.
12. SILVER, L. M.   Can. J. Phys. 29: 59.   1951.
13. SINCLAIR, W. K. and HOLLOWAY, A. F.   Nature, 167: 365.   1951.

THE ν_2 RAMAN BAND OF METHANE[1]

BY T. FELDMAN, J. ROMANKO,[2] AND H. L. WELSH

ABSTRACT

The doubly degenerate ν_2 Raman band of methane was photographed at a gas pressure of 2 atm. with a reciprocal linear dispersion of 10.5 cm.$^{-1}$ per mm. An analysis of the O and S branches gave $\nu_0 = 1533.6$, $B_0 = 5.270$, and $B_1 = 5.392$ cm.$^{-1}$. When the Raman data are combined with the infrared data of Burgess, Bell, and Nielsen, the effect of the Coriolis interaction of ν_2 with ν_4 is seen to be a splitting of the rotational levels of the upper vibrational state of ν_2 into two sets, each of which can be represented by an effective value of B_1. The Raman O, S and the infrared P (strong), Q, R (weak) transitions terminate in states with $B_1 = 5.392$ cm.$^{-1}$; the Raman P, Q, R and the infrared P (weak), R (strong) transitions terminate in states with $B_1 = 5.322$ cm.$^{-1}$.

INTRODUCTION

The four normal vibrations of the methane molecule are all active in the Raman effect. The totally symmetric ν_1 band, a single sharp line, and the triply degenerate ν_3 band, with extensive rotational structure, were first observed by Dickinson, Dillon, and Rasetti (6). More detail of the ν_3 band has been obtained recently (14). The doubly degenerate ν_2 band and the second triply degenerate band, ν_4, have been observed in the liquid (12, 5), the latter being extremely weak. The unresolved ν_2 band has been photographed at low dispersion with gaseous methane (15).

According to the selection rules for a tetrahedral molecule only the triply degenerate vibrations are active in infrared absorption. The most recent study of the ν_3 band is by Boyd, Thompson, and Williams (1), using high spectral resolution. The ν_4 band was observed by Nielsen and Nielsen (11), and analyzed by Childs and Jahn (3). A weak absorption at 6.3 μ, first noted by Coblentz (4), has been examined at high dispersion by Burgess, Bell, and Nielsen (2), and interpreted as the forbidden fundamental ν_2 made active through Coriolis interaction with ν_4. A detailed discussion of the complex structure of this band has not yet been given.

In spite of the many experimental and theoretical investigations of methane the interpretation of the finer details of the spectrum and the determination of the molecular constants leave much to be desired. This situation arises from the complicated rotation-vibrational interactions which are not fully understood. Even the rotational constant, $B_0 = h/8\pi^2cI_0$, from which the moment of inertia I_0 and the dimensions of the molecule in its ground vibrational state can be evaluated, is not accurately known. Since the methane molecule is a spherical top there is no rotational spectrum and the totally symmetric ν_1 band is a purely vibrational transition. The Raman and infrared ν_3 bands might be expected to yield a good value for B_0; however, the analyses of these bands have shown that the simple energy formulae, taking into ac-

count the Coriolis interaction between the mutually degenerate vibrational forms, do not explain adequately the observed rotational structure. The value $B_0 = 5.253$ cm.$^{-1}$, considered to give the best analysis of the ν_3 Raman band (14), is open to criticism. In their analysis of the infrared ν_3 band Boyd, Thompson, and Williams used the value $B_0 = 5.245$ cm.$^{-1}$, derived indirectly from the measurements of Ginsburg and Barker (8) on the infrared spectrum of monodeuteromethane.

The ν_2 Raman band offers the possibility of a more accurate determination of B_0. There is no Coriolis interaction between the mutually degenerate components, and the interaction with ν_4, although great enough to impart infrared activity to the band, might not make the Raman band unamenable to analysis. In the study of the ν_3 band with ultraviolet excitation (14) weak spectrograms of the ν_2 band were also obtained, and these indicated a normal structure for the band. Although the over-all intensity of the ν_2 band is only one-sixth that of the ν_3 band (15), the improved Raman source with visible excitation used in the present investigation permitted the band to be photographed readily at high dispersion.

EXPERIMENTAL

The Raman source and spectrograph, which have been described (16), can be used to photograph rotation-vibrational spectra of gases with a reciprocal linear dispersion of 10.5 cm.$^{-1}$ per mm. and a practical resolution of about 1 cm.$^{-1}$. Methane gas from a commercial cylinder, 99% pure, was condensed at liquid air temperature and allowed to evaporate slowly to give a pressure of two atmospheres in the Raman tube. Hg4358 was used for excitation of the ν_2 band. Without a filter the band was overlapped to some extent by the strong ν_3 band excited by Hg4047. The spectrogram of the ν_2 band used for measurement was obtained in an exposure time of 45 hr. with a sodium nitrite filter to remove Hg4047 from the exciting light. A microphotometer trace of this spectrogram is shown in Fig. 1.

The frequency shifts of the Raman lines were measured using comparison iron arc lines as standards and the value 22,938.04 cm.$^{-1}$ for the frequency of Hg4358. The measurements were made on the density trace obtained with a Leeds and Northrup microphotometer. The Raman shifts given in Table I are the averages of two reductions of the spectrum by different observers.
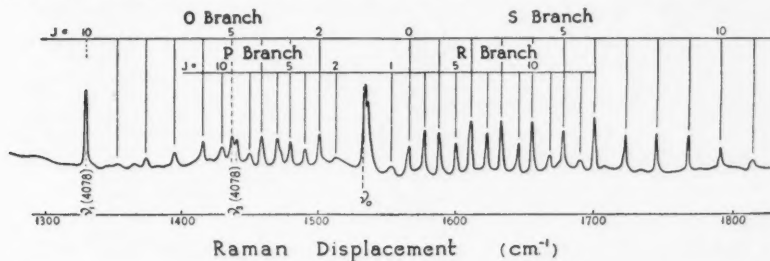

FIG. 1. Microphotometer trace of the ν_2 Raman band of methane excited by Hg4358.

TABLE I

OBSERVED FREQUENCIES IN THE ν_2 BAND OF CH_4

Raman spectrum		Infrared spectrum†		Assignment‡
Frequency (cm.⁻¹)	Relative intensity*	Frequency (cm.⁻¹)	Relative intensity*	
1359.1	0			$O^\beta(9)$
1380.5	1			$O^\beta(8)$
		1402.6	1	$P^\beta(17)$
1401.1	1			$O^\beta(7)$
		1404.7	3	$P^\beta(16)$
		1405.8	2	$P^\alpha(14)$
		1407.5	1	$P^\beta(15)$
		1411.3	2	—
		1412.4	3	$P^\alpha(13)$
		1416.5	1	$P^\beta(14)$
		1418.2	4	$\left.\right\}P^\beta(13)$
		1418.6	3	
1420.4	3			$O^\beta(6)$
		1421.1	1	$P^\alpha(12)$
		1425.9	6	$P^\beta(12)$
		1429.2	2	$P^\alpha(11)$
		1433.3	7	$P^\beta(11)$
1434.0	2	1436.1	1	$P^\alpha(10)$
		1441.1	6	$P^\beta(10)$
		1443.8	3	$P^\alpha(9)$
		1491.1	8	$P^\beta(9)$
1451.5	1	1452.6	2	$P^\alpha(8)$
		1457.2	7	$P^\beta(8)$
		1459.8	2	—
1460.6	3			$P^\alpha(7)$; $O^\beta(4)$
		1463.3	3	$P^\alpha(7)$
		1464.1	2	—
		1465.9	7	$P^\beta(7)$
1472.3	3	1473.0	4	$P^\alpha(6)$
		1474.7	7	$P^\beta(6)$
1481.7	3			$P^\alpha(5)$; $O^\beta(3)$
		1482.5	2	$P^\alpha(5)$
		1483.9	3	$P^\beta(5)$
1491.7	2	1492.2	3	$P^\alpha(4)$
		1493.7	4	$P^\beta(4)$
1501.8	3			$P^\alpha(3)$; $O^\beta(2)$
		1502.9	2	$P^\beta(3)$
1516.5	0			$P^\alpha(2)$
1534.3	10			$Q^\alpha_{max.}$
		1535.5	8	$Q^\beta(3)$
		1536.1	8	$Q^\alpha(5)$
1536.7	9			$Q^\alpha_{max.}$
		1536.7	8	$Q^\beta(4)$
		1537.8	10	$Q^\beta(5)$
		1538.2	9	$Q^\alpha(8)$
		1539.4	10	$Q^\beta(6)$; $Q^\alpha(9)$
		1540.9	9	$Q^\alpha(10)$
		1541.2	10	$Q^\beta(7)$
		1542.3	8	$Q^\alpha(11)$
		1543.2	10	$Q^\beta(8)$
		1545.7	10	$Q^\beta(9)$
		1548.4	9	$Q^\beta(10)$
		1550.9	6	$Q^\beta(11)$
		1553.9	6	$Q^\beta(12)$
		1556.8	4	$Q^\beta(13)$
1558.2	1	1558.2	2	$R^\alpha(1)$

TABLE I (*Concluded*)

Raman spectrum		Infrared spectrum†		Assignment‡
Frequency (cm.$^{-1}$)	Relative intensity*	Frequency (cm.$^{-1}$)	Relative intensity*	
		1560.0	3	$Q^\beta(14)$
		1565.3	2	$R^\alpha(2)$
1565.8	4			$S^\beta(0)$
		1566.8	2	$R^\beta(2)$
		1576.4	4	$R^\beta(3)$
1577.1	5	1576.9	3	$R^\alpha(3)$
1587.6	4			$R^\alpha(4); S^\beta(1)$
		1588.0	4	$R^\alpha(4)$
		1589.8	3	$R^\beta(4)$
1599.3	3	1599.3	4	$R^\alpha(5)$
		1601.7	2	$R^\beta(5)$
1610.3	6			$R^\alpha(6); S^\beta(2)$
		1610.7	7	$R^\alpha(6)$
		1614.2	2	$R^\beta(6)$
		1619.7	1	—
		1621.0	2	—
1621.8	4	1622.1	5	$R^\alpha(7)$
		1626.5	5	$R^\beta(7)$
		1630.5	1	—
1632.0	7			$R^\alpha(8); S^\beta(3)$
		1632.2	2	$R^\alpha(8)$
		1633.3	4	—
		1635.1	1	—
		1639.5	3	$R^\beta(8)$
		1641.5	1	—
		1643.3	1	—
1644.9	3	1644.9	5	$R^\alpha(9)$
		1652.6	5	$R^\beta(9)$
1654.3	6			$S^\beta(4); R^\alpha(10)$
		1654.6	4	$R^\alpha(10)$
		1656.3	4	—
		1663.0	2	—
		1665.7	4	$R^\beta(10)$
1667.6	1	1667.9	2	$R^\alpha(11)$
		1669.4	1	—
		1676.9	1	$R^\alpha(12)$
1677.0	4			$S^\beta(5); R^\alpha(12)$
		1678.8	4	$R^\beta(11)$
		1693.0	1	$R^\beta(12)$
1694.8	1	1696.0	0	$R^\alpha(13)$
1699.9	7			$S^\beta(6)$
		1700.9	1	$R^\alpha(14)$
		1706.7	0	$R^\beta(13)$
		1715.4	1	—
1723.0	4			$S^\beta(7)$
1746.5	4			$S^\beta(8)$
1770.5	2			$S^\beta(9)$
1793.7	0			$S^\beta(10)$

*The intensities are estimated on a scale of 10 to 0 from the microphotometer trace of the Raman band and from the recorder trace of the infrared band.
†The infrared data are taken from Burgess, Bell, and Nielsen (2).
‡In the assignments for blended lines the transition with the higher calculated intensity is given first.

DISCUSSION

From Fig. 1 the ν_2 Raman band appears to be a normal rotation-vibrational band with O, P, Q, R, and S branches corresponding to the selection rule

$\Delta J = 0$, ± 1, ± 2. However, some evidence of perturbation is present, especially in the lines of the P branch. A comparison of the P and R Raman frequencies with the corresponding infrared frequencies measured by Burgess, Bell, and Nielsen and reproduced in Table I shows that, although the Raman frequencies are present in the infrared band, they do not always correspond to the strongest infrared lines. In general, the infrared band shows much more evidence of perturbation than the Raman band; this is not surprising since the infrared band owes its intensity entirely to the Coriolis interaction with ν_4, and transitions to the most perturbed rotational states would probably give rise to the strongest lines.

The appearance of the Raman band encourages one to attempt an analysis using the usual formula for rotational energy terms

$$F_v(J) = B_v J(J+1) - D_v J^2(J+1)^2, \quad J = 0, 1, 2, \ldots ,$$

which is appropriate for unperturbed states of the doubly degenerate vibration. The O and S lines ($\Delta J = \pm 2$) extend over a greater range of frequencies than the P and R lines and are therefore more suitable for the determination of the molecular constants. The O and S lines form a single series which can be represented by the formula

$$\Delta \nu = \left[\nu_0 + \frac{3}{4}(B_1 - B_0) - \frac{9}{16}(D_1 - D_0) \right] + \left[(B_1 + B_0) - \frac{3}{2}(D_1 + D_0) \right] m$$
$$+ \left[\frac{1}{4}(B_1 - B_0) - \frac{11}{8}(D_1 - D_0) \right] m^2 - \frac{1}{2}(D_1 + D_2) m^3 - \frac{1}{16}(D_1 - D_0) m^4,$$

where $m = 2J+3$, $J = 0, 1, 2, \ldots$, for the S branch and $m = -2J+1$, $J = 2, 3, 4, \ldots$, for the O branch. With the assignment of J values as given in Table I, the observed frequencies of 16 O and S lines which are unblended with P and R lines were used to calculate the coefficients in the above formula by a regression method. The following values of the constants were obtained: $\nu_0 = 1533.6$, $B_0 = 5.270$, $B_1 = 5.392$, $D_0 = 2.85 \times 10^{-4}$, and $D_1 = 2.00 \times 10^{-4}$ cm.$^{-1}$. The value of B_0 is somewhat higher than those values previously determined and quoted in the Introduction. The values of D_0 and D_1 do not differ greatly from the value, 1.96×10^{-4} cm.$^{-1}$, calculated from the theoretical formula of Shaffer, Nielsen, and Thomas (13).

The comparatively high value of B_1 obtained from the analysis is a consequence of the marked convergence of the band towards lower frequency shifts. The convergence towards lower frequencies is also present in the infrared and has been discussed by Burgess, Bell, and Nielsen. The Coriolis interaction between ν_2 and ν_4 leads to a mutual repulsion of the levels with the same J in the two vibrational states. Since ν_2 ($= 1533.6$ cm.$^{-1}$) is greater than ν_4 ($= 1306$ cm.$^{-1}$) the rotational levels of ν_2 are raised and those of ν_4 depressed from their normal positions. The fact that the Raman O and S lines can be accurately represented by an effective B_1 value shows that the perturbation of the ν_2 rotational levels is proportional on the average to $J(J+1)$.

When the molecular constants determined from the O and S branches were used to calculate the frequencies of the P and R lines, it was found that the calculated frequencies deviated widely from the observed Raman frequencies;

the observed lines converge much less rapidly than the calculated lines. However, when the calculated frequencies were compared with the infrared data a surprising result was obtained: the calculated P frequencies coincide with *strong* lines in the infrared P branch and the calculated R frequencies coincide with *weak* lines in the infrared R branch. A systematic analysis of both the Raman and infrared bands was therefore undertaken.

The values of B_0 and D_0 determined from the Raman O and S lines were used to calculate $F_0(J)$, the rotational levels of the ground vibrational state. The levels, $F_1(J)$, of the $v_2 = 1$ vibrational state were then determined from the observed frequencies, ν, by the equation

$$F_1(J') = \nu - \nu_0 + F_0(J''),$$

where ν_0, the frequency of the band origin, was taken as 1533.6 cm.$^{-1}$. The assignment of J values for the Raman band presented no difficulty but some judgment was required in dealing with the more complex infrared band. In particular, two series of infrared P and R lines were identified; these are designated *strong* and *weak*. When the values of $F_1(J)/J(J+1)$ were plotted against $J(J+1)$ the distribution of points shown in Fig. 2 was obtained.
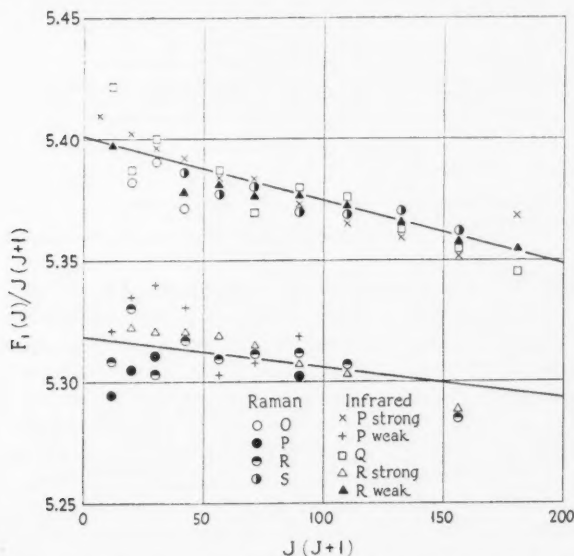
FIG. 2. Analysis of the Raman and the infrared ν_2 bands. Values of $F_1(J)/J(J+1)$, calculated from the observed frequencies assuming the ground state constants $\nu_0 = 1533.6$, $B_0 = 5.270$, and $D_0 = 2 \times 10^{-4}$ cm.$^{-1}$, are plotted against $J(J+1)$.

Although there is some scatter, especially at low J values, it is clear that the points define two straight lines, indicating that each of the states $F_1(J)$ is split into two components. If the energy terms are assumed to have the form

$$F_1(J) = B_1 J(J+1) - D_1 J^2(J+1)^2,$$

and the superscripts α and β are used to designate the lower and the higher of the two components respectively, a least squares analysis of the data plotted in Fig. 2 gives $B_1{}^\alpha = 5.318$, $D_1{}^\alpha = 1.4 \times 10^{-4}$, $B_1{}^\beta = 5.401$, and $D_1{}^\beta = 2.6 \times 10^{-4}$ cm.$^{-1}$.

The transitions terminating in the upper rotational level, J', indicated by this analysis are shown schematically in Fig. 3. Of the 10 branches which
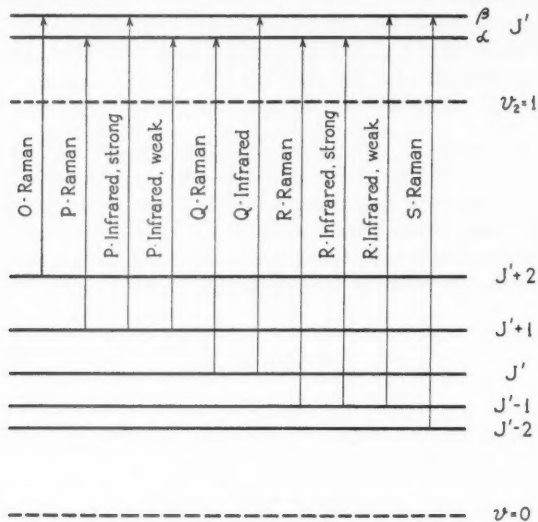

FIG. 3. Schematic diagram of the transitions observed in the Raman and the infrared ν_2 bands.

could be identified, five terminate in the α substates and five in the β substates. Although the Raman Q branch was not resolved into discrete lines, the fact that it is degraded towards higher frequencies much more rapidly (Fig. 1) than the infrared Q branch (Table I) shows that the α upper states are involved in its production. There is some indication that the infrared Q branches contain a closely spaced series corresponding to the Raman Q branch; these lines are tentatively assigned as $Q^\alpha(J)$ lines in Table I. When the same transition occurs in both the infrared and the Raman spectrum the infrared frequency is generally slightly higher than the Raman frequency; this might be ascribed to a systematic error in the infrared frequencies which, according to Burgess, Bell, and Nielsen, can be as great as 1 cm.$^{-1}$. Of the 83 lines observed by these authors all but 14 could be given assignments in the above analysis. The results of the analysis can be summarized as follows. In the Raman spectrum the selection rule $\Delta J = 0, \pm 1$ holds for the α substates and $\Delta J = \pm 2$ for the β substates. In the infrared spectrum the selection rule $\Delta J = 0, \pm 1$ holds for both the α and the β substates.

The reason for the type of doubling observed in the $v = 1$ state of the ν_2 vibration is not clear. Burgess, Bell, and Nielsen point out that the Hamiltonian for tetrahedrally symmetric molecules contains terms involving ν_2

which are of the same kind as those which produce l-type doubling in axially symmetric molecules. A detailed theoretical treatment of this type of perturbation is very desirable. It should also be noted that the calculations of Jahn (10) on the perturbation of ν_4 by ν_2 might be extended to determine directly the perturbation of the rotational levels of ν_2.

Since the interaction of ν_2 with ν_4 does not appear to preclude the analysis of the O and S branches with the usual rotational energy formula, it is considered that the value $B_0 = 5.270$ cm.$^{-1}$ is probably a fairly accurate value of the rotational constant of the ground vibrational state of methane. Using the atomic constants as given by Du Mond and Cohen (7) this B_0 value gives 1.091_0Å for the length of the C—H bond. These values of B_0 and r_0 are not inconsistent with those calculated from Ginsburg and Barker's measurement of the line spacing in the parallel bands of CH_3D if the more recent atomic constants are used in the reduction. A calculation with the newer constants gives $B_0 = 5.263$ instead of 5.245 cm.$^{-1}$, as calculated by Herzberg (9) and used by Boyd, Thompson, and Williams in their analysis of the ν_3 band of methane.

The values of the fundamental vibrational frequencies of methane, summarized in Table II, are considered to be the most accurate available at present.

TABLE II

FUNDAMENTAL FREQUENCIES (1–0 TRANSITIONS) OF GASEOUS METHANE

Assignment	$\nu_{vac.}$ (cm.$^{-1}$)	Source
$\nu_1(a_1)$	2916.5	Raman effect (14)
$\nu_2(e)$	1533.6	Raman effect (this investigation)
$\nu_3(f_2)$	3018.7 3018.8	Raman effect (14) Infrared absorption (1)
$\nu_4(f_2)$	1306	Infrared absorption (3)

REFERENCES

1. Boyd, D. R. J., Thompson, H. W., and Williams, R. L.   Proc. Roy. Soc. (London), A, 213: 48. 1952.
2. Burgess, J. S., Bell, E. E., and Nielsen, H. H.   J. Opt. Soc. Amer. 43: 1058.   1953.
3. Childs, W. H. J. and Jahn, H. A.   Proc. Roy. Soc. (London), A, 169: 451.   1939.
4. Coblentz, W. W.   Carnegie Inst. Wash. Publ. No. 35: 166.   1905.
5. Crawford, M. F., Welsh, H. L., and Harrold, J. H.   Can. J. Phys. 30: 81.   1952.
6. Dickinson, R. G., Dillon, R. T., and Rasetti, F.   Phys. Rev. 34: 582.   1929.
7. Du Mond, J. W. M. and Cohen, E. R.   Revs. Mod. Phys. 25: 691.   1953.
8. Ginsburg, N. and Barker, E. F.   J. Chem. Phys. 3: 668.   1935.
9. Herzberg, G.   Molecular spectra and molecular structure. II. Infrared and Raman spectra of polyatomic molecules. D. Van Nostrand Company, Inc., New York.   1945.
10. Jahn, H. A.   Proc. Roy. Soc. (London), A, 168: 469, 495.   1938.
11. Nielsen, A. H. and Nielsen, H. H.   Phys. Rev. 48: 864.   1935.
12. Rank, D. H., Shull, E. R., and Axford, D. W. E.   J. Chem. Phys. 18: 116.   1950.
13. Shaffer, W. H., Nielsen, H. H., and Thomas, L. H.   Phys. Rev. 56: 895.   1939.
14. Stoicheff, B. P., Cumming, C., St. John, G. E., and Welsh, H. L.   J. Chem. Phys. 20: 498. 1952.
15. Welsh, H. L., Crawford, M. F., Thomas, T. R., and Love, G. R.   Can. J. Phys. 30: 577. 1952.
16. Welsh, H. L., Stansbury, E. J., Romanko, J., and Feldman, T.   J. Opt. Soc. Amer. In press.

Adiabatic Oscillations in Liquid Helium II

This letter presents some preliminary results of experiments performed in this laboratory to test the prediction of Robinson (2) that "adiabatic oscillations" could be produced in liquid helium II.

The essentials of the apparatus are shown in Fig. 1. From the appearance of the optical interference fringes and the measured flow rates of helium II into the beaker, it is concluded that the separation of the optical flats is about 10^{-4} cm. When the apparatus is filled with liquid helium II the beaker can be lowered into the surrounding liquid, the "bath", and liquid helium drawn in through C by means of a thermal gradient produced with the heater.
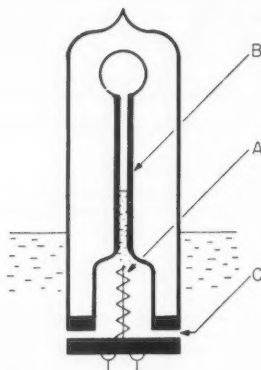
FIG. 1. The helium beaker and its vacuum jacket. A heater and main volume; B capillary; C annular gap between optical flats.

The helium meniscus can be arranged to appear in the capillary B at a convenient level, where it will remain at a constant equilibrium fountain-height above the level of the bath liquid provided no temperature changes occur in bath or beaker. To ensure a steady meniscus level the temperature of the outer helium dewar is carefully controlled by a temperature stabilizing bridge, Boyle and Brown (1).

If these equilibrium conditions are suddenly disturbed in one of the ways described below, the liquid helium meniscus in B will quickly take up a new position, and then oscillate about that position. The various ways in which oscillations have been initiated are:

(1) Quickly raising or lowering the beaker,

(2) Passing a short pulse of current through the heater,

(3) Suddenly changing the amount of radiation incident on the beaker, or altering the bath temperature.

These oscillations are strongly damped, and in general they die down before the meniscus has begun the return towards its initial equilibrium position. The meniscus returns to its initial level at a rate which is determined by the heat leakage from beaker to bath. This rate varies from experiment to experiment, depending on the condition of the beaker, and in cases where it is large, the meniscus has returned a considerable distance toward the starting position before the oscillations cease.

A stroboscopic light was used to give a shadowgraph image of the meniscus, which was recorded by an oscillograph camera with a continuously moving film. The thermal disturbance due to the use of the stroboscopic lamp was arranged to be a minimum, commensurate with obtaining a usable photographic record.

146

The record of the oscillation obtained on the film was measured, and the meniscus level plotted against time measured by the "frame number" of the image (see Fig. 2).

The oscillation was initiated by discharging a condenser through the heater, thereby introducing 8000 ergs into the beaker. The stroboscope operated at 50 flashes per second with a dissipation of 0.04 joules per flash.
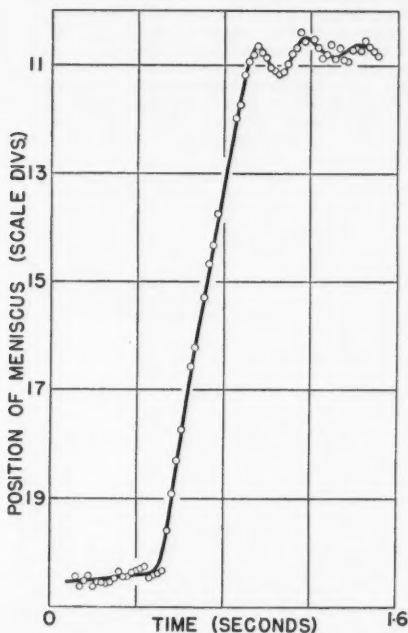

FIG. 2. Plot of adiabatic oscillation at 1.74°K. Amplitude approximately 0.2 mm. maximum, and frequency approximately 4.5 cycles per second.

As a measure of the thermal contact between the beaker and bath, the rate of return of the meniscus to its original level has been measured and in the case of Fig. 2 the relaxation time was 100 sec.

With such a limited number of periods the frequency measurement can only be used for an approximate check on Robinson's prediction (see Fig. 1 of his paper). The observed value of ω_a (the adiabatic angular frequency) at 1.74°K. is 28 radians/sec. and ω_0 (the calculated isothermal frequency at 0°K.) for the present apparatus is 0.7 radian/sec. so that $\omega_a/\omega_0 = 40$. When allowance is made for the volume of the beaker containing helium (cf. Robinson's "h") the experimental value of ω_a/ω_0 is still higher, which puts it noticeably above Robinson's curve, but this matter cannot be settled at present. However the order of magnitude of the frequency and the general behavior indicate that these are the adiabatic oscillations envisaged by Robinson.

Further experiments are in progress and a more complete account will be published later.

1. BOYLE, W. S. and BROWN, J. B. Rev. Sci. Instr. 25: 359. 1954.
2. ROBINSON, J. E. Phys. Rev. 82: 440. 1951.

F. D. MANCHESTER*
DEPARTMENT OF PHYSICS,
UNIVERSITY OF BRITISH COLUMBIA,
VANCOUVER, B.C.

*Holder of a National Research Council Studentship 1952–54.

On Anomalies in the Absorption of Cosmic Rays in Lead

Irregularities in the absorption curve of cosmic rays in lead have been reported by several authors (1, 2, 3, 4, 7, 8, 10, 11), using counter telescopes. More recently, other workers (5, 6, 9), who were looking specifically for these anomalies, failed to find them. Our initial experiment (7), using a single triple coincidence telescope and point-by-point scanning of the absorption curve, yielded an anomalous maximum as shown in curve I (Fig. 1). Since it was felt that day-by-day fluctuations might have been responsible for this maximum, we have repeated our experiment, determining four points on the absorption curve simultaneously. Curve II, so obtained, shows no evidence for any anomalies and supports the careful measurements of Heyland and Duncanson (6).

The telescope configurations used in the present experiment are shown in the inset of Fig. 1. The counters were of the external cathode type, with plateaus of about 250 volts and an average slope of 0.02% per volt. Arrangement (a) defines four triple coincidence telescopes with the side counters in anticoincidence. The rates 123–7, 124–7, 125–7, and 126–7 were recorded. The anticoincidence counters were used to reduce the differences in the telescope apertures and the
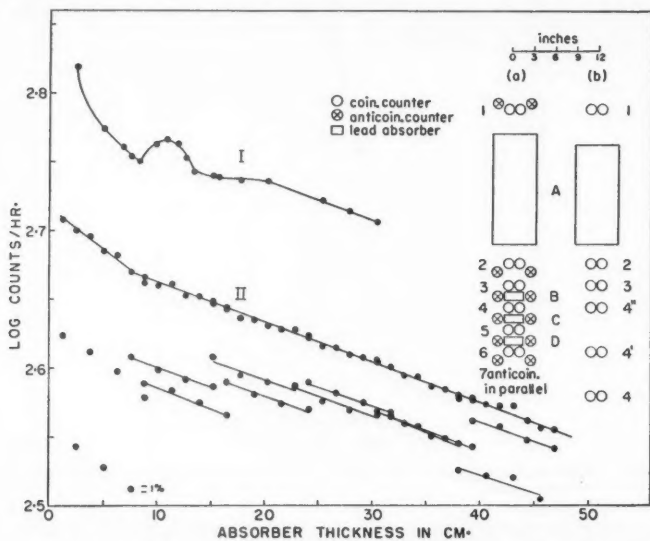

FIG. 1. Absorption curve of cosmic rays in lead, showing telescope arrangement inset.

errors due to scattering and side showers. The results for four absorber thicknesses were obtained simultaneously by placing 1 in. thickness of lead at B, C, and D. Absorber A was varied to give both overlapping and adjacent four-point segments of the absorption curve. The rates of the different telescopes were normalized to that of 123–7 by multiplying by the appropriate "geometry factors". These factors, which are the ratios of the counting rates of the telescopes with no absorbers in positions B, C, or D, were constant in time and independent of lead thickness in position A. Since the factors were also directly proportional to the ratios of the angular apertures, it was concluded that the efficiencies of the telescopes were equal and the factors were truly geometric.

The final results of the absorption measurements are also presented in Fig. 1. The four-point segments, corrected for geometry only, are shown in the lower part of the graph. Each point is based on approximately 15,000 counts. The internal consistency of the points defining a segment is much better than that expected from statistical considerations because the counting rates are not completely independent. However, the variations in the segments are, in some cases, much greater than would be expected from random counting. These large differences are interpreted as being caused by atmospheric fluctuations, a source of error that was not taken into account in our earlier work. The end points of the segments were fitted together to give curve II of Fig. 1. No corrections for accidental and shower rates were made since these were at all times less than 1% of the observed rate.

Since in our earlier work the absorber was above the telescope (as for 234 of arrangement (*b*) in Fig. 1) while in the present work it was within the telescope (as for 123 of the same arrangement) it was felt that perhaps the anomalies observed were dependent on the position of the absorber relative to the telescope. However, it was found that the ratio of the rate 123 to the rate 234 taken simultaneously was independent of absorber thickness, provided the cross-sectional area of the absorber was sufficient to fill the apertures of both telescopes. The ratio became strongly dependent on absorber thickness unless this requirement was strictly adhered to.

It is concluded that within 1% there is no anomaly in the cosmic ray absorption curve for lead thicknesses up to 45 cm. Moreover, these experiments suggest that the previously observed anomalies could easily have been created by insufficient attention to the proper arrangement of absorbers or to changes in atmospheric conditions.

1. ABD EL-WAHAB KHALIL, M. Nuovo cimento, 9: 1248. 1952.
2. AIYA, S. V. C. Nature, 153: 375. 1950.
3. FENYVES, E. and HAIMAN, O. Nature, 165: 244. 1950.
4. GEORGE, E. P. and APPAPILLAI, V. Nature, 155: 726. 1945.
5. HEYLAND, G. R. and DUNCANSON, W. E. Nature, 167: 895. 1951.
6. HEYLAND, G. R. and DUNCANSON, W. E. Proc. Phys. Soc. (London), A, 66: 33. 1953.
7. KEECH, G. L. M.Sc. Thesis, McMaster University, Hamilton, Ont. Oct. 1952.
8. KELLERMANN, E. W. and WESTERMAN, K. Proc. Phys. Soc. (London), A, 62: 356. 1949.
9. KENNEDY, W. L. Australian J. Phys. 6: 500. 1953.
10. MAZZOLLI DE MATHOV, E. Nature, 167: 192. 1951.
11. SWANN, W. F. G. and MORRIS, P. F. Phys. Rev. 72: 1262. 1947.

RECEIVED JANUARY 17, 1955.
DEPARTMENT OF PHYSICS,
HAMILTON COLLEGE,
MCMASTER UNIVERSITY,
HAMILTON, ONTARIO.

G. L. KEECH*
F. GULBIS

*Holder of a National Research Council Studentship 1954–55.

CANADIAN JOURNAL OF PHYSICS

Notes to Contributors

Manuscripts

(i) *General.* Manuscripts, in English or French, should be typewritten, double spaced, on paper $8\frac{1}{2} \times 11$ in. **The original and one copy are to be submitted.** Tables and captions for the figures should be placed at the end of the manuscript. Every sheet of the manuscript should be numbered.

Style, arrangement, spelling, and abbreviations should conform to the usage of this journal. Names of all simple compounds, rather than their formulas, should be used in the text. Greek letters or unusual signs should be written plainly or explained by marginal notes. Superscripts and subscripts must be legible and carefully placed.

Manuscripts should be carefully checked before they are submitted; authors will be charged for changes made in the proof that are considered excessive.

(ii) *Abstract.* An abstract of not more than about 200 words, indicating the scope of the work and the principal findings, is required, except in Notes.

(iii) *References.* References should be listed **alphabetically by authors' names,** numbered, and typed after the text. The form of the citations should be that used in this journal; in references to papers in periodicals, titles should not be given and only initial page numbers are required. All citations should be checked with the original articles and each one referred to in the text by the key number.

(iv) *Tables.* Tables should be numbered in roman numerals and each table referred to in the text. Titles should always be given but should be brief; column headings should be brief and descriptive matter in the tables confined to a minimum. Vertical rules should be used only when they are essential. Numerous small tables should be avoided.

Illustrations

(i) *General.* All figures (including each figure of the plates) should be numbered consecutively from 1 up, in arabic numerals, and each figure referred to in the text. The author's name, title of the paper, and figure number should be written in the lower left corner of the sheets on which the illustrations appear. Captions should not be written on the illustrations (see Manuscripts (i)).

(ii) *Line Drawings.* Drawings should be carefully made with India ink on white drawing paper, blue tracing linen, or co-ordinate paper ruled in blue only; any co-ordinate lines that are to appear in the reproduction should be ruled in black ink. Paper ruled in green, yellow, or red should not be used unless it is desired to have all the co-ordinate lines show. All lines should be of sufficient thickness to reproduce well. Decimal points, periods, and stippled dots should be solid black circles large enough to be reduced if necessary. Letters and numerals should be neatly made, preferably with a stencil (**do NOT use typewriting**) and be of such size that the smallest lettering will be not less than 1 mm. high when reproduced in a cut 3 in. wide.

Many drawings are made too large; originals should not be more than 2 or 3 times the size of the desired reproduction. In large drawings or groups of drawings the ratio of height to width should conform to that of a journal page but the height should be adjusted to make allowance for the caption.

The original drawings and one set of clear copies (e.g. small photographs) are to be submitted.

(iii) *Photographs.* Prints should be made on glossy paper, with strong contrasts. They should be trimmed so that essential features only are shown and mounted carefully, with rubber cement, on white cardboard with no space or only a **very** small space (less than 1 mm.) between them. In mounting, full use of the space available should be made (to reduce the number of cuts required) and the ratio of height to width should correspond to that of a journal page $(4\frac{3}{4} \times 7\frac{1}{2}$ in.); however, allowance must be made for the captions. Photographs or groups of photographs should not be more than 2 or 3 times the size of the desired reproduction.

Photographs are to be submitted in duplicate; if they are to be reproduced in groups one set should be mounted, the duplicate set unmounted.

Reprints

A total of 50 reprints of each paper, without covers, are supplied free. Additional reprints, with or without covers, may be purchased.

Charges for reprints are based on the number of printed pages, which may be calculated approximately by multiplying by 0.6 the number of manuscript pages (double-spaced typewritten sheets, $8\frac{1}{2} \times 11$ in.) and including the space occupied by illustrations. An additional charge is made for illustrations that appear as coated inserts. The cost per page is given on the reprint requisition which accompanies the galley.

Any reprints required in addition to those requested on the author's reprint requisition form must be ordered officially as soon as the paper has been accepted for publication.

Contents